P66Shc-mediated reactive oxygen species and autophagy disrupts brain microvascular endothelial cell function in response to hyperglycemia

Lin Wang (lin.wang@whu.edu.cn)
Wuhan University

Mengzhen Yang
Wuhan University

Chao Wu
Wuhan University

Hanyang Hu
Wuhan University

Lulu Ji
Wuhan University

Rujie Lai
Wuhan University

Min Peng
Medical School of Nanjing University

Shenghe Huang
Yunnan Institute of Pediatrics, Kunming Children's Hospital

Research Article

Keywords: high glucose, ZO-1, Human brain microvascular endothelial cells, P66Shc

Posted Date: April 7th, 2022

DOI: https://doi.org/10.21203/rs.3.rs-1512054/v1

Abstract

Diabetes mellitus is a metabolic disease characterized by hyperglycemia, which can lead to serious central nervous system complications. The blood-brain barrier(BBB) is essential for maintaining the environmental stability of the central nervous system. Hyperglycemia may cause blood-brain barrier dysfunction and lead to central nervous system complications, but the mechanism is not clear. To explore the molecular mechanism of BBB injury caused by high glucose (HG), we hypothesize that p66Shc damaged BBB by promoting ROS production and autophagy. Human brain microvascular endothelial cells (HBMEC) were treated with different concentrations of glucose, Mito-tempo (MT), autophagy inhibitor (3-MA), autophagy inducer rapamycin (RAP), and P66Shc siRNA. Western blot was used to detect the expression of LC3, P62, ZO-1, claudin-5, and P66Shc in HBMEC. Autophagosomes were observed by transmission electron microscopy (TEM). Immunofluorescence staining was used to observe the expression of ZO-1, occludin, and ROS. The autophagy level was enhanced by HG. HG decreased the expression of ZO-1 and increased the expression of P66Shc and ROS. Inhibition of ROS levels under HG reversed the high level of autophagy induced by HG and increased the expression of ZO-1. The autophagy level was negatively correlated with the ZO-1 expression in HG. In HG, inhibit the expression of P66Shc reduced the ROS and autophagy levels and increased the ZO-1 expression. HG increased the autophagy level and destroyed the integrity of the tight junctions between HBMEC. Silencing P66Shc repaired HG damaged-HBMEC by inhibiting ROS production and reducing autophagy. To explore the molecular mechanism of BBB injury caused by high glucose (HG), we hypothesize that p66Shc damaged BBB by promoting ROS production and autophagy.

Introduction

The diabetes mellitus pandemic has reached alarming magnitudes, affecting more than 415 million people worldwide and accounting for one death every six seconds in 2015. If the current trends in diabetes prevalence continue, it is expected to reach 642 million by 2040 (Cho, 2016). Diabetes is a metabolic disease characterized by hyperglycemia, leading to various complications (Kurniawan et al., 2019, Alexandru et al., 2016, Liu et al., 2018). Diabetes-related vascular complications are among the most common complications in prolonged diabetic patients, and their mechanisms are complicated. One of the most common risk factors is hyperglycemia, which contributes to endothelial dysfunction (Alexandru et al., 2016). HBMEC is connected by different types of tight and adherens junctions, forming the BBB, which limits blood cells and pathogens into the brain (Winkler et al., 2011). Zonula occludens-1 (ZO-1) protein is one of the most critical tight junctions between HBMEC, restricting small molecular substances' passing. It is essential for maintaining the function of HBMEC (Schwayer et al., 2019). Occludin is the first integral membrane protein discovered within the tight junctions (TJ) of HBMEC, including the BBB (Zlokovic, 2008). Claudin-5 is also one of the critical tight junctions between adjacent endothelial cells in the BBB (Jiao et al., 2011, Nitta et al., 2003). Oxidative stress plays a pivotal role in the development of diabetic microvascular complications. The metabolic abnormalities of diabetes cause mitochondrial superoxide overproduction in HBMEC. Increased intracellular ROS destroy the tight

junctions between HBMEC (Giacco and Brownlee, 2010), but its molecular mechanism is still not fully understood. P66Shc is a member of the SHC family, which regulates a variety of metabolic activities. Furthermore, p66Shc is a redox enzyme that generates mitochondrial ROS (hydrogen peroxide) (Giorgio et al., 2005). Autophagy is a complex process to maintain cell homeostasis. It is a process of cell self-synchronization in which part of the cytoplasm is isolated in double or multi-membrane vesicles (autophagosomes) and then delivered to the lysosome undergoes extensive degradation (Galluzzi and Green, 2019). Dysfunctional mitophagy leads to the accumulation of dysfunctional mitochondria. Therefore, it causes increasing the production of ROS (Festa et al., 2018). Hyperglycemia is associated with intestinal barrier disruption (Thaiss et al., 2018), but it is less known about its role in BBB, and the mechanism is poorly understood. Whether p66Shc regulates the autophagy level through ROS and affects the structure and function of HBMEC in HG (HG) has not yet been reported. Altogether, these data suggest potential interactions between p66Shc, autophagy, ROS, and HG in HBMEC.

In the present study, we decipher a pathway linking autophagy dysfunctions, mitochondrial oxidative stress, disruption of tight junction integrity, and p66Shc causing HBMEC dysfunction.

Materials And Methods

Cells culture

The human brain microvascular endothelial cell line was cultured as described in the previous studies (Chi et al., 2012). The human brain microvascular endothelial cell line was cultured in RPMI 1640 medium (Gibco, Grand Island, NY, USA) containing 10% heat-inactivated fetal bovine serum, two mM glutamine, one mM sodium pyruvate, streptomycin (100 μg/mL), and penicillin G (50 μg/mL) at 37°C in 5% CO_2.

Western blotting.

Proteins were extracted from HBMEC, lysed using RIPA, which contains protease and phosphatase inhibitors, followed by centrifugation at 13,000 rpm for 15 min at 4°C. SDS-PAGE separated the samples. After blocking with 5% non-fat milk diluted in PBS, the membranes were incubated with primary antibody GAPDH, LC3, p62, ZO-1 overnight at 4°C. After being washed, the membranes were incubated with secondary antibody (1: 5000, Proteintech, Wuhan, Hubei, China). Image J software was used for the semi-quantification of protein expression.

Antibodies and reagents

Rabbit anti-ZONAB (bs-12985R, Bioss; 1:100); fluorescent secondary antibody (goat anti-rabbit Alexa 488), Lipofectamine 2000 (Invitrogen; Thermo Fisher Scientific Life Sciences), rabbit FITC-conjugated antibodies (Proteintech, Wuhan, Hubei, China) the HRP-conjugated secondary antibody (1: 5000,

Proteintech, Wuhan, Hubei, China), and Mito-TEMPO (MT; ALX-430-150-M005, Enzo Life Sciences). Rabbit anti-ZO-1 (13663, Cell Signaling; 1:400); rabbit anti-LC3 (Sigma-Aldrich; 1:2000), rabbit anti-p62/SQSTM1 (PM045, MBL; 1:200); rabbit anti-GAPDH (2118, Cell Signaling Technology; 1:10,000); rabbit anti-Occludin (91131, Cell Signaling;1:200); rabbit anti-phospho-Src Family (Tyr416) (6943, Cell Signaling; 1:1000); rabbit anti-Claudin-5 (bsm-52933R, Bioss; 1:500).

RNA isolation and reverse transcription

Total RNA of HBMEC was extracted using TRIzol Reagent (Invitrogen; Thermo Fisher Scientific Life Sciences, Waltham, MA). RNA was further purified from the TRIzol extract with 20% chloroform, centrifuged, and precipitated from the resulting water phase with isopropanol. After RNA extraction, the reverse transcription was synthesized using Revert Aid TM First Strand cDNA Synthesis Kit from Fermentas according to the manufacturer's instructions using random primer.

Real-time polymerase chain reaction

Each reaction contained cDNA. The PCR primers were designed with Primer Premier 5.0 software, and β-Actin was used as a reference gene. qPCR was performed on iQ5 Real-Time PCR Detection System (Bio-Rad, USA) using SYBR Green Real-Time PCR Master Mix (TOYOBO CO., LTD, Japan). P66shc specific primers (Forward: AATTTGGGCCTCTTGTACAGTT, Reverse: TACCTCACAGGCCTAGGCGAGG). ZO-1 specific primers (Forward: CGGTCCTCTGAGCCTGTAAG, Reverse: GGATCTACATGCGACGACAA).

siRNA Transfection

HBMEC was incubated with siRNA targeting p66Shc (sense: 5'-AUGAGUCUCUGUCAUCGCUtt-3'; antisense: 5'-AGCGAUGACAGAGACUCAUtt-3') (GenePharma) for four h in a confocal dish, used Lipofectamine 2000 (Invitrogen; Thermo Fisher Scientific Life Sciences), followed by growing in standard growth medium in 24h. Scrambled siRNA (sense: 5'-GAUCAUACGUGCGAUCAGA-3'; antisense: 5'-UCUGAUCGCACGUAUGAUC-3' were used as negative controls (NC group).

Immunofluorescence microscopy

After being exposed to HG for 24 hours with or without Mito-TEMPO (MT), a mitochondrial ROS inhibitor, cells were grown on L-lysine coated 5% BSA were washed three times with PBS and fixed with 4% paraformaldehyde in PBS at room temperature for 20 min. After being blocked with 5% BSA for 60 min, cells were incubated with the primary antibodies ZO-1 in the blocking solution at 4℃ overnight. After being washed three times, cells were incubated with a fluorescent secondary antibody (goat anti-rabbit Alexa 488) for ZO-1. After washing, the cell was stained with DAPI. All samples were examined under a fluorescence microscope or confocal microscope.

Electron microscope

HBMEC was fixed in 4% PFA/0.1% glutaraldehyde in 100 nm sodium cacodylate, at pH 7.43, dehydrated, and embedded in LR-White resin. We viewed the grids on transmission electron microscope at 80 kV. We identified autophagic vacuoles by a double membrane structure of autophagosomes according to standard criteria.

ROS detection.

Cells were treated with DCFH-DA (10μM for 30min at 37°C) in live-cell imaging at 37℃. After washing, the cells were subsequently analyzed by confocal microscopy. The fluorescence intensity was quantified using the open-source cell image analysis software Cell Profiler 63, as described below.

Statistical Analysis

All experiments were performed in triplicate and repeated at least three times. Statistically significant differences between groups were determined using two-tailed one-way ANOVA, followed by a Student–Newman–Keuls test or Student t-test. $P < 0.05$ was considered statistically significant.

Results

Hyperglycemia induces autophagy in HBMEC.

To test whether elevated glucose levels were causally involved in HBMEC autophagy, we treated HBMEC with different glucose concentrations (5.5mM, 11mM, 16.5mM, 22mM, and 27.5mM). The p62 protein, a selective autophagy protein, carried the substrate degraded by interacting with LC3 in autophagosomes. So the degradation of p62 protein was a vital sign of autophagolysosome formation (Fujimoto et al., 2017, Kameyama et al., 2017, Lamark et al., 2017, Yao et al., 2017). Indeed, autophagy levels increased in HG-treated cells. The western blot results showed that glucose treatment increased LC3II/LC3I but decreased SQSTM1/p62 in a concentration-dependent manner. Therefore, the 5.5 mM group was selected as the control group in the subsequent experiments, and the 27.5 mM group was selected as the HG group (Fig. S1). Compared with the control group, the high-glucose group showed a significant increase in the LC3-II/LC3-I protein level and a significant decrease in the protein level of p62 (Fig. 1A, B), suggesting that the high-glucose environment raise the autophagy level of HBMEC. Transmission electron microscopy results further showed that the number of autophagosomes was increased in the HG group compared with the control group (Fig. 1C). After treatment with mannitol (osmotic pressure control, 27.5mM), cells exhibited the same levels of LC3-II/LC3-I, p62, and ZO-1 compared with the physiological blood glucose level (control) group (P□0.05) (Fig. 1 D, E). In summary, these data showed that HG plays an essential role in regulating autophagy.

Hyperglycemia induces HBMEC disruption.

To determine whether glucose acted directly on HBMEC to affect BBB function, we used an in vitro system of cultured HBMEC exposed to HG concentrations in the culture medium. We assessed tight junction integrity through immunofluorescence analysis of ZO-1 and occludin staining patterns. HG treatment significantly increased the mRNA ($P< 0.05$) and protein expression of ZO-1 (Fig. S2 and 2 A, B). Immunofluorescence microscopy experiment showed that the structure of ZO-1 decreased in HG treated cells (Fig. 2C). Indeed, HG treatment also resulted in the dysfunction of brain microvascular epithelial adherence junctions and altered appearance of cell-cell junctions (Fig. 2 C and S3 A). The western blotting experiment suggested that the level of ZO-1 protein and claudin-5 protein were decreased in HG group (Fig. 2 A, B, D, and E). Together, these experiments establish HG as a direct and specific cause for HBMEC dysfunction and disruption of cell-cell junctions.

Hyperglycemia induces trans-epithelial flux of HBMEC via ROS.

To explore whether HG affected the ROS to destroy the TJ protein and mitochondrial structure in HBMEC, we used western blot, immunofluorescence staining, and transmission electron microscopy to detect ROS, ZO-1 protein level, and mitochondrial structure under HG environment. The immunofluorescence staining results showed that ROS's fluorescence intensity in the HG group was significantly higher than in the control group, suggesting that HG increases ROS level in HBMEC (Fig.3A). HG altered the structure of ZO-1 and occludin and enhanced the trans-epithelial flux of HBMEC (Fig. 3 B, S3 A). HG treatment also resulted in mitochondria dysfunction and up-regulating autophagy (Fig. 3 C, D, and E).

After using mitochondria-localized-oxygen scavenger Mito-TEMPO (MT), the fluorescence intensity of ROS was significantly reduced, suggesting that MT can reduce the level of ROS (Fig. 3A). Western blot showed that the level of LC3-II/LC3-I in the MT+HG group was significantly reduced than the HG group, and the protein level of p62 was significantly increased than the HG group (Fig. 3C-D). Indeed, MT-treated HBMEC enhanced the structure of ZO-1 and occludin (Fig. 3 B and S3 A) and decreased mitophagy and dysfunction of mitochondria (Fig. 3, C, D, and E).

Together, these experiments establish ROS as a direct cause for mitochondria dysfunction and disruption of cell-cell junctions.

Negative feedback loop between ZO-1 and autophagy

To corroborate whether autophagy influenced ZO-1 expression, we used rapamycin (an autophagy agonist) and 3-MA (an autophagy inhibitor) to modulate autophagy levels. HBMEC was treated with HG, rapamycin, and 3-MA. Western blot showed that compared with the HG group, the level of LC3II/LC31 increased, and the level of p62 decreased, and ZO-1 protein decreased in the rapamycin group (cells

treated with HG and rapamycin). In contrast, the level of LC3II/LC31 reduced, and the p62 and ZO-1 protein level increased in the 3-MA group (HBMEC treated with HG and 3-MA) (Fig. 4 A-B). Electron microscopy (EM) shows more autophagic vacuoles in HG conditions or rapamycin group than the 3-MA group (Fig. 4C). Together, these results suggested that autophagy affects cell-cell junctions and decreases ZO-1 expression in HG conditions.

Silencing of p66Sch increases tight junction in HG-treated HBMEC

First, we discovered that HG-treated HBMEC increased protein levels of P66Shc compared with the control group (Fig. 5 A, B). To determine whether glucose acted directly on p66Shc to affect autophagy and ZO-1 expression, we silenced p66Shc and detected the level of ROS, claudin-5, ZO-1 protein, and autophagy. Therefore, siRNA against p66Shc treated HBMEC reduced the mRNA level of p66Shc within 24h compared with siScr (Fig. 5 C). Indeed, we detected that the Si-p66Shc group reduced ROS level within 24h (Fig.5 D), and decreased autophagy level (Fig. 5E, F) compared with NC (HG+siScr) group. Together, these data suggest that HG-mediated disruption of HBMEC was potentially caused by an increase of p66Shc. P66Shc induces autophagy and ROS to aggravate the destruction of the HBMEC.

Discussion

BBB is a diffusion barrier between blood and brain tissue composed of endothelial cells, astrocyte end-feet, and pericytes. The integrity of the BBB structure plays a vital role in maintaining the normal physiological function of brain tissue (Ballabh et al., 2004). Serum glucose is among the most strictly controlled physiological variables of organismal homeostasis (Thaiss et al., 2018). Hyperglycaemia causes harmful consequences on the endothelium, vascular smooth muscle cells, and macrophages, leading to thrombosis and fibrinolysis, which result in the formation of atherosclerotic plaques. Hyperglycaemia is associated with high cardiovascular-related mortality and morbidity both in T1DM and T2DM (Laakso and Kuusisto, 2014). Only a weak relationship has been found between hyperglycemia and BBB; however, hyperglycemia strongly predicts stroke, amputation, and peripheral vascular disease (Laakso and Kuusisto, 2014). Those complications affect the brain, as well as increase the risks of infection and mortality. Hyperglycemia is associated with intestinal barrier disruption (Thaiss et al., 2018), but it is less known about its role in HBMEC, and the mechanism is poorly understood. In our study, we used immunofluorescence and western blot to detect the levels of TJ protein in HG-treated HBMEC. Our results show that HG could significantly decrease TJ protein levels between brain endothelial cells, suggesting that HG enhanced the trans-epithelial flux of BBB.

ROS is defined as an oxygen-containing molecule, including superoxide, hydrogen peroxide, and hydroxyl radical, among others. ROS generally derived from exogenous oxidants or intracellular aerobic metabolism. It plays an essential physiological role in preventing foreign substances invasion and regulating in-vivo biological processes (Li et al., 2016). ROS also plays an important pathophysiology

role. The balance between oxidation and anti-oxidation sustaining exists in physiological conditions. In the brain, there is a defense system including enzymatic antioxidant defense systems and non-enzymatic antioxidant defense systems to protect the brain from oxidation damage. Oxidation and antioxidants are in dynamic equilibrium. Once mitochondria suffer from oxidative stress, they produce a large amount of ROS (Geto et al., 2020, Kaludercic and Di Lisa, 2020). Oxidative glucose metabolism leads to the production of ROS. Hyperglycaemia is proposed to lead to large amounts of ROS (Stumvoll et al., 2005). Therefore, to explore whether HG affected the ROS to destroy the TJ protein and the mitochondrial structure in HBMEC, we use western blot, immunofluorescence staining, and transmission electron microscopy to detect the level of ROS, ZO-1 protein, occludin protein, and mitochondrial structure under HG environment. Our results show that HG induced-oxidative stress causes damaged mitochondria, which enhances the trans-epithelial flux of HBMEC and mitophagy.

Autophagy plays a vital role in many physiological processes and is a degradative pathway that involves delivering cytoplasmic components, including proteins, organelles, and invaded microbes, to the lysosome for digestion (Levine and Kroemer, 2008). Oxidative stress, nutritional and energy deficiency, infection, and protein accumulation can induce autophagy (Green and Levine, 2014). Some studies show that ROS induces autophagy to protect cells from apoptosis or necrosis (Huang et al., 2011). To test whether ROS is causally involved in HBMEC autophagy levels, we treated HBMEC with MT + HG. Indeed, our results suggested that ROS induces autophagy.

The p66shc protein has two shorter isoforms called p52shc and p46shc, encoded by the Shc1 locus from various exon arrangements at the 50 end. P52shc and p46shc are encoded using different translation initiation sites (Ciciliot and Fadini, 2019). P66Shc is a protein adaptor of the SHC family, which is involved in regulating various metabolic pathways. One of the most strongly affected pathways by hyperglycemia in our study involves p66Shc protein, which has been implicated as a critical regulator of many cell functions. P66shc played a significant role in mitochondrial ROS production (Ciciliot and Fadini, 2019). However, it has not been reported whether p66Shc affects the integrity of HBMEC by regulating autophagy in HG. Therefore, in this study, we have identified glucose as an orchestrator of HBMEC function. Hyperglycemia-mediated p66Shc markedly interfered with homeostatic epithelial integrity, leading to abnormal autophagy and ROS. Our results indicate that up-regulation p66Shc causes up-regulation of autophagy and ROS, followed by alterations in the structure of cell-cell junctions.

Collectively, our findings provide a potential molecular explanation for HG-mediated disruption of BBB. BBB dysfunction plays a vital role in diabetes-mediated central nervous system diseases such as stroke, vascular dementia, and memory loss. The changes in glucose level (hyperglycemia) affect the transport of glucose, amino acids, and other substances in the BBB, affecting the integrity of the BBB, and are closely related to the oxidative stress of microvessels in the CNS. However, due to the complex underlying pathogenesis of diabetes-related CNS complications, the pathogenesis needs to be further investigated. Furthermore, the link that we highlight between p66 and BBB integrity may provide a mechanistic basis for ROS and autophagy influencing BBB function. Ultimately, our results may present the starting point

for harnessing glucose metabolism or other regulators of BBB integrity as potential therapeutic targets in the prevention and alleviating of CNS complications.

Declarations

Data availability statement

The raw data supporting the conclusions of this manuscript will be made available by the authors, without undue reservation, to any qualified researcher.

Conflict of Interest

The authors declared no conflict of interest.

Funding

This study was supported by the National Natural Science Foundation of China (No. 82171681).

Acknowledgments

Thanks for the equipment (Leica-LCS-SP8-STED) provided by the structural center of the School of Basic Medical Sciences, Wuhan University.

References

1. ALEXANDRU, N., BADILA, E., WEISS, E., COCHIOR, D., STĘPIEŃ, E. & GEORGESCU, A. 2016. Vascular complications in diabetes: Microparticles and microparticle associated microRNAs as active players. *Biochem Biophys Res Commun,* 472**,** 1-10.
2. BALLABH, P., BRAUN, A. & NEDERGAARD, M. 2004. The blood-brain barrier: an overview: structure, regulation, and clinical implications. *Neurobiol Dis,* 16**,** 1-13.
3. CHI, F., BO, T., WU, C. H., JONG, A. & HUANG, S. H. 2012. Vimentin and PSF act in concert to regulate IbeA+ E. coli K1 induced activation and nuclear translocation of NF-κB in human brain endothelial cells. *PLoS One,* 7**,** e35862.
4. CHO, N. H. 2016. Q&A: Five questions on the 2015 IDF Diabetes Atlas. *Diabetes Res Clin Pract,* 115**,** 157-9.
5. CICILIOT, S. & FADINI, G. P. 2019. Modulation of Obesity and Insulin Resistance by the Redox Enzyme and Adaptor Protein p66(Shc). *Int J Mol Sci,* 20.
6. FESTA, B. P., CHEN, Z., BERQUEZ, M., DEBAIX, H., TOKONAMI, N., PRANGE, J. A., HOEK, G. V., ALESSIO, C., RAIMONDI, A., NEVO, N., GILES, R. H., DEVUYST, O. & LUCIANI, A. 2018. Impaired autophagy bridges lysosomal storage disease and epithelial dysfunction in the kidney. *Nat Commun,* 9**,** 161.
7. FUJIMOTO, C., IWASAKI, S., URATA, S., MORISHITA, H., SAKAMAKI, Y., FUJIOKA, M., KONDO, K., MIZUSHIMA, N. & YAMASOBA, T. 2017. Autophagy is essential for hearing in mice. *Cell Death Dis,* 8**,**

e2780.

8. GALLUZZI, L. & GREEN, D. R. 2019. Autophagy-Independent Functions of the Autophagy Machinery. *Cell,* 177**,** 1682-1699.
9. GETO, Z., MOLLA, M. D., CHALLA, F., BELAY, Y. & GETAHUN, T. 2020. Mitochondrial Dynamic Dysfunction as a Main Triggering Factor for Inflammation Associated Chronic Non-Communicable Diseases. *J Inflamm Res,* 13**,** 97-107.
10. GIACCO, F. & BROWNLEE, M. 2010. Oxidative stress and diabetic complications. *Circ Res,* 107**,** 1058-70.
11. GIORGIO, M., MIGLIACCIO, E., ORSINI, F., PAOLUCCI, D., MORONI, M., CONTURSI, C., PELLICCIA, G., LUZI, L., MINUCCI, S., MARCACCIO, M., PINTON, P., RIZZUTO, R., BERNARDI, P., PAOLUCCI, F. & PELICCI, P. G. 2005. Electron transfer between cytochrome c and p66Shc generates reactive oxygen species that trigger mitochondrial apoptosis. *Cell,* 122**,** 221-33.
12. GREEN, D. R. & LEVINE, B. 2014. To be or not to be? How selective autophagy and cell death govern cell fate. *Cell,* 157**,** 65-75.
13. HUANG, J., LAM, G. Y. & BRUMELL, J. H. 2011. Autophagy signaling through reactive oxygen species. *Antioxid Redox Signal,* 14**,** 2215-31.
14. JIAO, H., WANG, Z., LIU, Y., WANG, P. & XUE, Y. 2011. Specific role of tight junction proteins claudin-5, occludin, and ZO-1 of the blood-brain barrier in a focal cerebral ischemic insult. *J Mol Neurosci,* 44**,** 130-9.
15. KALUDERCIC, N. & DI LISA, F. 2020. Mitochondrial ROS Formation in the Pathogenesis of Diabetic Cardiomyopathy. *Front Cardiovasc Med,* 7**,** 12.
16. KAMEYAMA, K., MOTOYAMA, K., TANAKA, N., YAMASHITA, Y., HIGASHI, T. & ARIMA, H. 2017. Induction of mitophagy-mediated antitumor activity with folate-appended methyl-β-cyclodextrin. *Int J Nanomedicine,* 12**,** 3433-3446.
17. KURNIAWAN, A. H., SUWANDI, B. H. & KHOLILI, U. 2019. Diabetic Gastroenteropathy: A Complication of Diabetes Mellitus. *Acta Med Indones,* 51**,** 263-271.
18. LAAKSO, M. & KUUSISTO, J. 2014. Insulin resistance and hyperglycaemia in cardiovascular disease development. *Nat Rev Endocrinol,* 10**,** 293-302.
19. LAMARK, T., SVENNING, S. & JOHANSEN, T. 2017. Regulation of selective autophagy: the p62/SQSTM1 paradigm. *Essays Biochem,* 61**,** 609-624.
20. LEVINE, B. & KROEMER, G. 2008. Autophagy in the pathogenesis of disease. *Cell,* 132**,** 27-42.
21. LI, R., JIA, Z. & TRUSH, M. A. 2016. Defining ROS in Biology and Medicine. *React Oxyg Species (Apex),* 1**,** 9-21.
22. LIU, Y., LI, M., ZHANG, Z., YE, Y. & ZHOU, J. 2018. Role of microglia-neuron interactions in diabetic encephalopathy. *Ageing Res Rev,* 42**,** 28-39.
23. NITTA, T., HATA, M., GOTOH, S., SEO, Y., SASAKI, H., HASHIMOTO, N., FURUSE, M. & TSUKITA, S. 2003. Size-selective loosening of the blood-brain barrier in claudin-5-deficient mice. *J Cell Biol,* 161**,** 653-60.

24. SCHWAYER, C., SHAMIPOUR, S., PRANJIC-FERSCHA, K., SCHAUER, A., BALDA, M., TADA, M., MATTER, K. & HEISENBERG, C. P. 2019. Mechanosensation of Tight Junctions Depends on ZO-1 Phase Separation and Flow. *Cell,* 179**,** 937-952.e18.
25. STUMVOLL, M., GOLDSTEIN, B. J. & VAN HAEFTEN, T. W. 2005. Type 2 diabetes: principles of pathogenesis and therapy. *Lancet,* 365**,** 1333-46.
26. THAISS, C. A., LEVY, M., GROSHEVA, I., ZHENG, D., SOFFER, E., BLACHER, E., BRAVERMAN, S., TENGELER, A. C., BARAK, O., ELAZAR, M., BEN-ZEEV, R., LEHAVI-REGEV, D., KATZ, M. N., PEVSNER-FISCHER, M., GERTLER, A., HALPERN, Z., HARMELIN, A., AAMAR, S., SERRADAS, P., GROSFELD, A., SHAPIRO, H., GEIGER, B. & ELINAV, E. 2018. Hyperglycemia drives intestinal barrier dysfunction and risk for enteric infection. *Science,* 359**,** 1376-1383.
27. WINKLER, E. A., BELL, R. D. & ZLOKOVIC, B. V. 2011. Central nervous system pericytes in health and disease. *Nat Neurosci,* 14**,** 1398-1405.
28. YAO, L., WANG, J., TIAN, B. Y., XU, T. H. & SHENG, Z. T. 2017. Activation of the Nrf2-ARE Signaling Pathway Prevents Hyperphosphatemia-Induced Vascular Calcification by Inducing Autophagy in Renal Vascular Smooth Muscle Cells. *J Cell Biochem,* 118**,** 4708-4715.
29. ZLOKOVIC, B. V. 2008. The blood-brain barrier in health and chronic neurodegenerative disorders. *Neuron,* 57**,** 178-201.

Figures

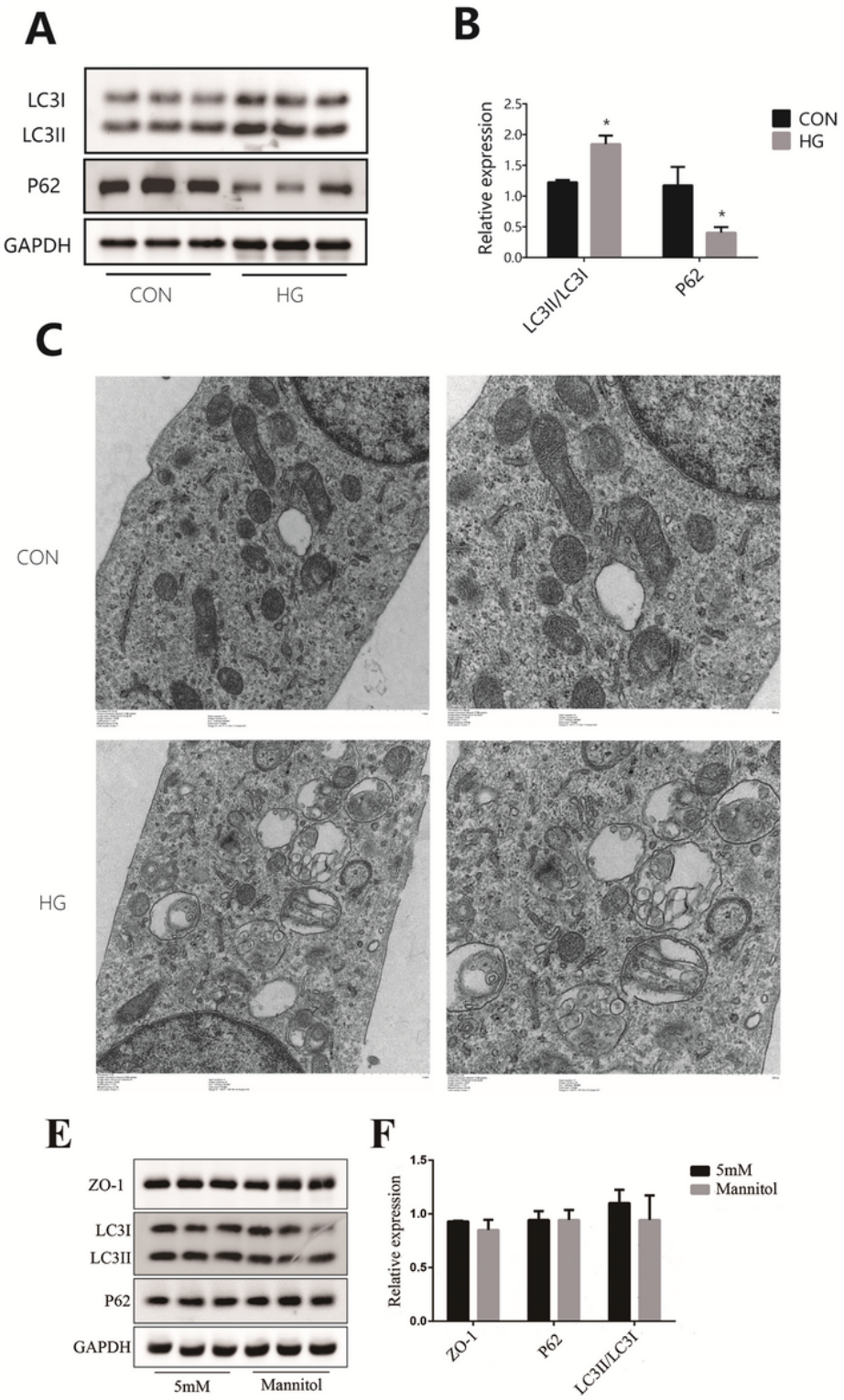

Figure 1

HG increases autophagy. (A-B) HBMEC was treated with glucose (5.5 mM, 27.5 mM) for 24 hours. P62 and LC3II/LC3I proteins were detected by western blot. 5.5 mM glucose treated- HBMEC was the control group (CON); 27.5 mM glucose treated- HBMEC was the HG group (HG). HG group vs. CON group indicates* $p<0.05$. (C) Autophagic vacuoles were viewed by electron microscopy (EM). Representative 7k electron micrographs (left) and 10k electron micrographs (right) of numbers of autophagic vacuoles per

cell. Autophagic vacuoles increased in the HG group than in the CON group. (D-E) The western blotting analysis demonstrated the expression of ZO-1, LC3, and p62 in cells treated with mannitol and glucose for 24 hours. Data are means ± SEM of 3 independent experiments conducted in triplicate. GAPDH, glyceraldehyde 3-phosphate dehydrogenase; *, P < 0.05.

Figure 2

HG disrupts TJ proteins. HG down-regulation of the protein of ZO-1. (A-B) Expressions of ZO-1 were measured by Western blot. ZO-1 protein decreased in the HG group than the CON group. (C) Representative fluorescence microscopy images of ZO-1, ZO-1 protein, were analyzed by confocal microscopy. ZO-1 protein decreased in the HG group than the CON group. (D-E) Representative western blotting bands of Claudin-5 and glyceraldehyde3-phosphate dehydrogenase (GAPDH). HG group vs. CON group indicates* p<0.05.

Figure 3

HG-damaged mitochondria induce oxidative stress, resulting in a decrease in ZO-1. Mitochondrial ROS scavenging ameliorates function in HBMEC (A) HBMEC was treated with 5.5 mM glucose (CON) and treated with 27.5 mM glucose (HG) for 24 hours, HBMEC was treated with 27.5 mM glucose and mitochondria-targeted antioxidant Mito-Tempo (MT, 10μM for 24h) in the culture medium for 24 hours (MT). (A) Representative fluorescence microscopy images of ROS. The HBMEC was treated with DCFH-DA (10μM for 30min at 37°C) to test ROS level. Moreover, the ROS level was analyzed by confocal microscopy. (B) Representative fluorescence microscopy images of ZO-1. Expressions of ZO-1 were measured by confocal microscopy in the same condition as mentioned in A; Nuclei counterstained with DAPI (blue). (C-D) Western blotting analyses of ZO-1, LC3II/LC3I, and P62 protein levels. (E)Representative electron micrographs show damaged mitochondria and mitophagy in CON, HG, and MT groups. Data are means ± SEM of 3 independent experiments conducted in triplicate. GAPDH, DAPI, *, P < 0.05.

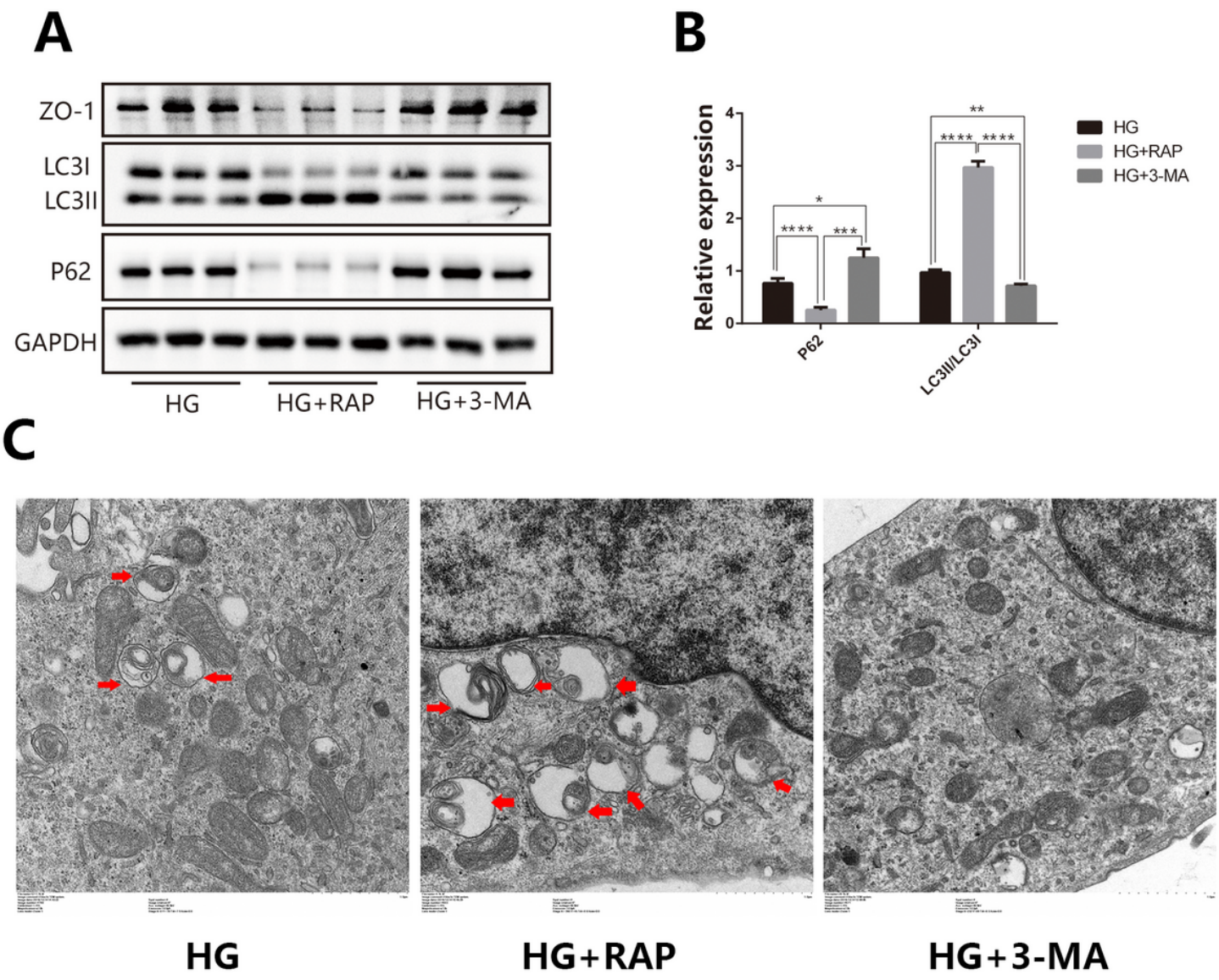

Figure 4

Inhibition of autophagy revealed ZO-1 increase; increased autophagy revealed ZO-1 decrease. A large autophagy cause dysfunction in HBMEC (A-B) HBMEC was treated with 27.5 mM glucose in the culture medium for 24 hours (HG). Moreover, HBMEC was treated with 27.5 mM glucose and rapamycin (200 nM for 2h) in the culture medium for 24 hours (HG+RAP). Furthermore, HBMEC was treated with 27.5 mM glucose and 3-MA (5mM for 2h) in the culture medium for 24 hours (HG+3-MA). Western blotting analyses ZO-1, P62, and LC3I/LC3II protein levels. (C) Autophagic vacuoles were viewed by electron microscopy in the same condition as A. Data are means ± SEM of 3 independent experiments conducted in triplicate. GAPDH, *, P < 0.05; **, P < 0.01; ***, P < 0.001, ****, P < 0.0001.

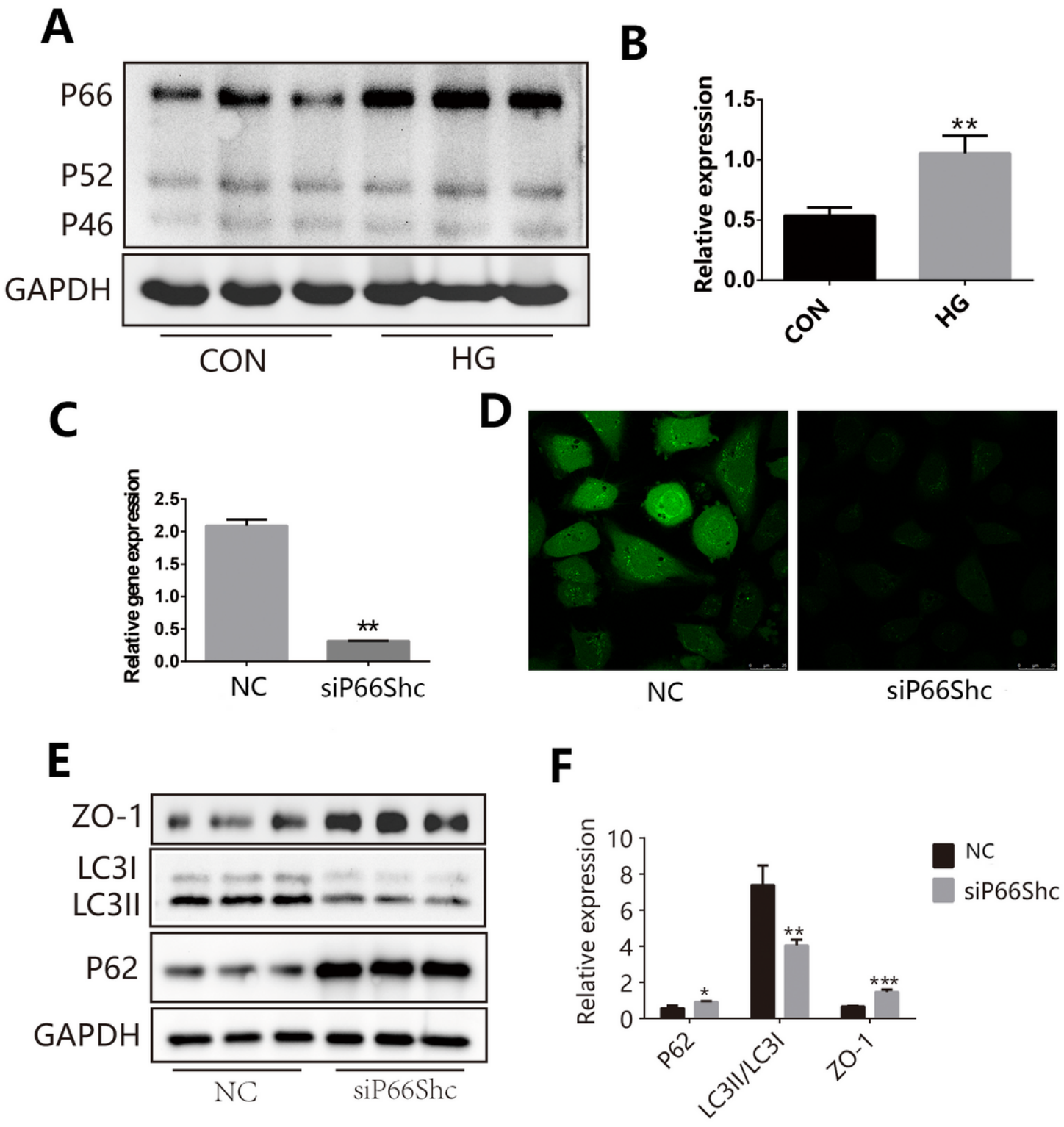

Figure 5

HG increases p66Shc that induces autophagy, P66Shc rise leads to a decreased tight junction; Inhibition of p66Shc decreases autophagy and increases ZO-1. P66Shc promotes HBMEC ROS and autophagy. (A-B) Western blotting analysis of p66Shc in HBMEC treated with 5.5 mM and 27.5 glucose for 24h. (C) Real-time polymerase chain reaction analysis of P66Shc mRNA in HBMEC treated with Scrambled siRNA(NC group) or P66Shc siRNA(siP66Shc group) in HG condition for 24h. (D) Representative

fluorescence microscopy images of ROS after silencing of p66Shc. HBMEC treated as C. And ROS level was analyzed by confocal microscopy. (E-F) The western blotting analysis demonstrated the expression of ZO-1, LC3II/LC3I, and p62 protein level after silencing p66Shc. Data are means ± SEM of 3 independent experiments. *, P < 0.05; **, P < 0.01; ***, P < 0.001.

Supplementary Files

This is a list of supplementary files associated with this preprint. Click to download.

- FigureS1.tif
- figureS2.tif